RSC Advances

PAPER

View Article Online
View Journal | View Issue

Cite this: *RSC Adv.*, 2016, **6**, 7897

Enhanced photovoltaic performance with co-sensitization of a ruthenium(II) sensitizer and an organic dye in dye-sensitized solar cells

Umer Mehmood,[ab] Ibnelwaleed A. Hussein,*[c] Khalil Harrabi,[ad] Nouar Tabet[e] and G. R. Berdiyorov[f]

Received 12th December 2015
Accepted 9th January 2016

DOI: 10.1039/c5ra26577k

www.rsc.org/advances

Co-sensitization is demonstrated to be an effective technique to enhance the efficiency of dye-sensitized solar cells, where an efficiency of 9.23% is achieved by mixing N3 and RK-1 dyes. The assembled solar cells are characterized by UV-vis absorption measurements, current–voltage characteristics, and electrochemical impedance spectroscopy. The co-sensitized solar cell shows an enhanced photovoltaic performance as compared to the devices sensitized by individual dyes. Upon optimization, the device made of 0.3 mM N3 + 0.2 mM RK-1 yielded J_{sc} = 18.1 mA cm^2, V_{oc} = 888 mV, FF = 57.44, and η = 9.23%. This performance is superior to that of solar cells sensitized with either N3 (6.10%) or RK-1 (5.82%) fabricated under the same conditions. The enhanced efficiency can be attributed to the decrease of the competitive light absorption by I^-/I_3^-, dye aggregation, and charge recombination.

1. Introduction

Solar energy is considered the most promising solution to abate climate change resulting from the uncontrolled use of fossil resources for energy generation.[1–5] At present, more than 40 billion tons of greenhouses gasses are emitted annually to the atmosphere.[6] Carbon dioxide emission from coal, oil, natural gas, cement manufacturing, and gas flaring were 43%, 33%, 18%, 5.3%, and 0.6%, respectively in 2012.[7–9] The development of an environmentally friendly and reliable energy technology is essential and photovoltaic (PV) technology permits direct conversion of sunlight into electrical power without the emission of greenhouse gasses and other polluting agents. The major hurdle limiting the large-scale deployment of PV technology remains the cost of silicon-based PV technology which is dominating the market currently. Thus, all R&D efforts at present are focused on ways to reduce the cost of power produced from solar energy. Dye-sensitized solar cells (DSSCs) emerged in the 1990s as a promising and cost-effective technology.[9]

The major component of the DSSCs is a dye, with the functionality of absorbing the incident solar energy and producing free photo-electron–hole pairs (excitons). The dye always adsorbs on the porous surface of a semiconducting layer such as TiO_2 that ensures charge separation and the transfer of electrons from the excited dye to one of the electrodes.[10,11]

However, the traditional sensitizers suffer from narrow absorption spectra, low absorption, and loss of energy absorb by the electrolyte, leading to low efficiencies of DSSCs based on them.[12] Therefore, a co-sensitization strategy was suggested and implemented to improve the performance of the DSSC.[13–16] Many co-sensitized systems have been successfully implemented to improve the performance of DSSCs, such as a ruthenium-based photosensitizers co-sensitized with metal free dyes,[17–19] porphyrin[20–22] or phthalocyanine[23–25] co-sensitized with an organic dye, and an organic dye co-sensitized with another organic dye.[26,27] Z. Wu *et al.*[28] used N719 with an organic dye (AZ5) and obtained an efficiency of 7.91%. Kuo-Chuan Ho *et al.* achieved an efficiency of 6.24% by co-sensitization of organic dyes (5c and SQ2).[29] Sharma *et al.* fabricated DSSCs by employing a ruthenium-based complex co-sensitized with an organic dye and reached an efficiency of 6.29%.[30]

In this work, a ruthenium-based complex N3 is co-sensitized with an organic dye RK-1 to enhance the photovoltaic performance of DSSCs. The structure and the chemical name of the two sensitizers are shown in Fig. 1. N3 is known to very efficiently photo-sensitize TiO_2 in the visible spectrum up to a wavelength of ~700 nm. But it relatively shows weaker absorption over ultraviolet spectrum.[31] On the other hand, RK-1

[a]*Center of Research Excellence in Renewable Energy (CoRE-RE), Research Institute (RI), King Fahd University of Petroleum & Minerals (KFUPM), P. O. Box 5050, Dhahran 31261, Kingdom of Saudi Arabia. E-mail: ihussein@qu.edu.qa*

[b]*Polymer and Process Engineering Department, University of Engineering & Technology, Lahore, Pakistan*

[c]*Gas Processing Center, College of Engineering, Qatar University, PO Box 2713, Doha, Qatar*

[d]*Department of Physics, KFUPM, P. O. Box 5050, Dhahran 31261, Kingdom of Saudi Arabia*

[e]*Qatar Environment and Energy Research Institute, Qatar Foundation Doha, Qatar*

[f]*Qatar Environment and Energy Research Institute, Hamad Bin Khalifa University, P. O. Box 5825, Doha, Qatar*

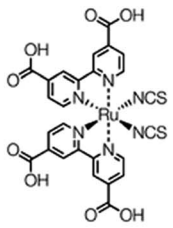

(a)

Cis-diisothiocyanato-bis (2, 2'-bipyridyl-4, 4'-dicarboxylic acid) ruthenium (II) [N3]

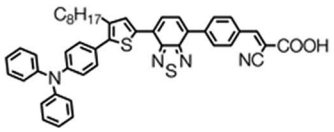

(b)

2-cyano-3-(4-(7-(5-(4- (diphenylamino) phenyl)-4- octylthiophen-2-yl) benzo[c] [1, 2, 5] thiadiazol-4-yl) phenyl) acrylic acid [RK-1]

Fig. 1 Structures and chemical names of N3 dye and RK-1.

consists of dissymmetric pi-conjugated bridge that contains an alkyls chain and an electron deficient unit localized close to the electron-withdrawing anchoring function and an electron-rich unit close to the aryl amine donating group. The introduction of a phenyl ring between acceptor benzothiadiazole (BTD) and the cyanoacrylic acid group stabilize the dye radical cation and decrease recombination.[32] Therefore, RK-1 could be an effective organic sensitizer for co-sensitization with N3 owing to its wide-ranging light absorption properties as well as good charge recombination resistance. The efficiency of the co-sensitized device is significantly enhanced as compared to that of solar cells sensitized with a single dye, with the overall efficiency of the 0.3 mM N3 + 0.2 mM RK-1 device improving to 9.23%.

2. Experimentation

Seven different solutions of composite dye *i.e.* 0.5 mM N3, 0.5 mM RK-1, 0.4 mM N3 + 0.1 mM RK-1, 0.3 mM N3 + 0.2 mM RK-1, 0.25 mM N3 + 0.25 mM RK-1, 0.2 mM N3 + 0.3 mM RK-1 and 0.1 mM N3 + 0.4 mM RK-1 were prepared in methanol.

2.1. Fabrication of DSSCs

The electrodes were prepared by tape casting TiO_2 paste (T/SP14451, Solaronix) on a conductive glass substrate (TCO22-7, Solaronix) and then annealed at 450 °C for 30 min. The thickness of TiO_2 film on a conductive glass substrate was measured by using cross-sectional images obtained from SEM (JEOL, 6610LV) (not shown in the manuscript). The average thickness of each film was 10 μm. The counter electrode was prepared by depositing a 5 nm platinum film on FTO glass substrate using a sputtering machine (Q150R sputter coater) at room temperature.

TiO_2 coated FTO glass substrates were immersed in dye solutions for 24 hours. After sensitization, unanchored dye molecules were detached by washing the sensitized samples with ethanol. The solar cells were assembled by using the photoanode, the counter electrode, a 60 μm sealing spacer (Meltonix 1170, Solaronix), and the electrolyte with 50 mM of the I^-/I_3^- redox couple in methoxypropionitrile (Iodolyte Z-50, Solaronix). The active area of the solar cell is 0.25 cm^2.

2.2. Device characterization

UV-vis spectra of both dye solutions and adsorbed on TiO_2 films were measured by a spectrophotometer (JASCO-670 UV/VIS). The current–voltage (*I–V*) characteristics of solar cells were measured with the help of IV-5 solar simulator (Sr #83, PV Measurement, Inc) at AM1.5G (100 mW cm^{-2}). Characterization with electrochemical impedance spectroscopy (EIS) was conducted under dark conditions employing a Bio-Logic SAS (VMP3, s/n: 0373), using an AC signal of 10 mV in amplitude, in the frequency range between 10 Hz and 500 kHz.

3. Results and discussion

The UV-vis absorption spectra of N3, RK-1, and N3 + RK-1 in methanol are shown in Fig. 2a. The broad peaks of N3 in the visible region at 528 and 394 nm are assigned to metal-to-ligand charge transfer (MLCT). The band in the UV region at 314 nm is assigned to intraligand (π–π*) charge-transfer transitions. Similarly, the RK-1 dye in methanol gives two distinct absorption bands: one band is in the 300–390 nm region due to π–π*

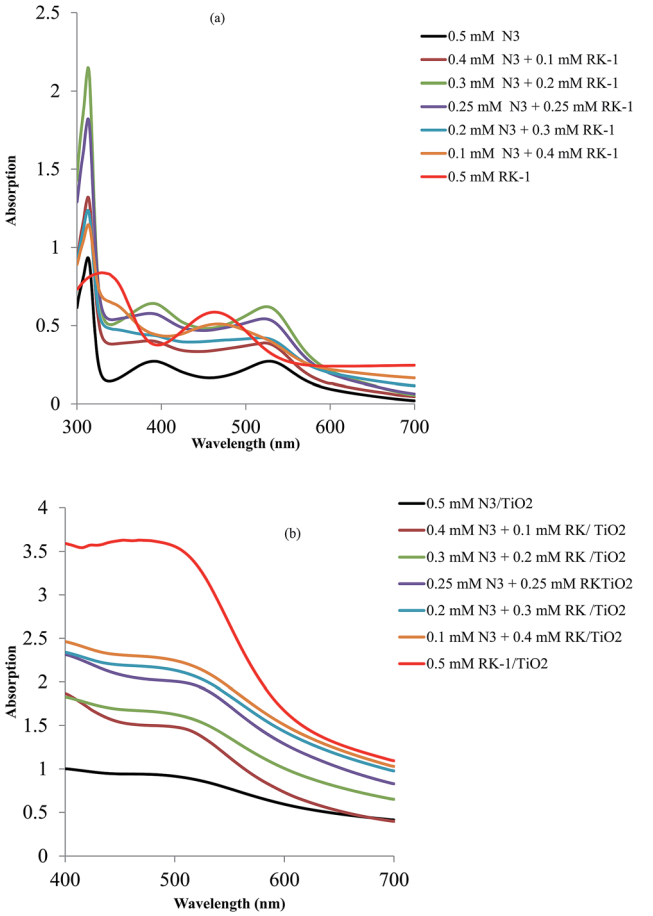

Fig. 2 UV-vis spectra of (a) dyes in methanol and (b) dyes anchored on TiO_2 films.

electron transitions of the conjugated molecules, and the second around 390–600 nm can be assigned to an intermolecular charge transfer (ICT) between the electron-donor and electron-acceptor anchoring moieties. In addition, the methanol solutions of N3 + RK-1 show much more intensive and broader bands as compared to N3 dye alone due to the synergistic effect of two dyes. The increase in absorptions are in the order of sample-3 > sample-4 > sample-2 > sample-5 > sample-6 > sample-1 > sample-7. The UV-vis absorption of RK-1, N3, and N3 + RK-1 anchored to TiO_2 films are illustrated in Fig. 2b. The maximum absorption peak of RK-1 in TiO_2 films is red shifted to 500 nm with respect to that in the solution owing to J-aggregation and interaction with the TiO_2 film.[14] Thus, RK-1 possesses much higher light harvesting ability in this region. Hence, it is expected that the loss of light absorption by I_3^- to will be compensated by the use of the co-sensitizer RK-1. The maximum absorption peak of N3 in the film is significantly blue-shifted to 514 nm compared to that in solution, which indicates that H-aggregation occurs for N3 adsorbed on the TiO_2 film.[21] However, upon co-sensitization with RK-1 in the TiO_2 film, the maximum absorption of N3 is red-shifted as compared to that of N3 alone in the film; but it is still blue-shifted as compared to that of N3 in solutions. This implies that both H-aggregation and J-aggregation[33,34] probably occurs for N3 under co-sensitization conditions. Fig. 2b shows that the absorption increases with the decrease of N3 concentration in the solution. It confirms that (under optimal conditions) the proposed co-sensitized thin films can absorb more photons than the individual sensitized TiO_2 films. Thus, light harvesting (LHE) efficiency can be improved by co-sensitization.

Fig. 3 shows the *I–V* characteristics of the TiO_2 based DSSCs, sensitized/co-sensitized with N3, RK-1, and N3 + RK-1. The photovoltaic parameters of DSSCs, *i.e.*, J_{sc}, V_{oc}, FF, and η, are summarized in Table 1. The results show that the N3 sensitized DSSC yielded a J_{sc} of 14.747 mA cm^{-2}, a V_{oc} of 786 mV, and FF of 52.6%, resulting in an efficiency of 6.10%. On the other hand, the RK-1 sensitized DSSC yielded a J_{sc} of 15.25 mA cm^{-2}, a V_{oc} of 758 mV, a FF of 51.430%, and an efficiency of 5.82%. Encouragingly, the co-sensitized DSSCs exhibit significantly improved efficiency as compared to that of the devices sensitized by N3 or RK-1 alone. Upon optimization, the device made of 0.3 mM N3 + 0.2 mM RK-1 yielded a J_{sc} = 18.1 mA cm^2, V_{oc} = 888 mV, FF = 57.44, and η = 9.23%. The improvement in efficiency is mainly due to an enhancement of the values of J_{sc} (18.1 mA cm^2) and V_{oc} (888 mV), which are strongly correlated to the intense light absorption in the visible region and reduced charge recombination, respectively. Since, the co-sensitization improves the LHE, it demonstrates that higher the LHE, greater will be the photocurrent and hence more efficiency. Moreover, the improvement in efficiency can also be attributed to the fact that the co-sensitizer effectively overcomes the competitive light absorption by I^-/I_3^-, avoids dye aggregation, and reduces charge recombination.

EIS, which measures the current response at different frequencies of the applied AC voltage, was used to study the charge transfer resistance of the cells. The Nyquist plots for the DSSCs studied and the equivalent circuit is shown in Fig. 4a. Typically, normal impedance spectra of DSSCs consist of three arcs (semicircles). The first semicircle represents the interfacial resistance at the counter electrode/electrolyte interface (R_1), second represents the interfacial resistance at the photoanode/electrolyte interface (R_2) or (R_{ct}), and the third represents the impedance due to the diffusion process of I^-/I_3^- redox couple in

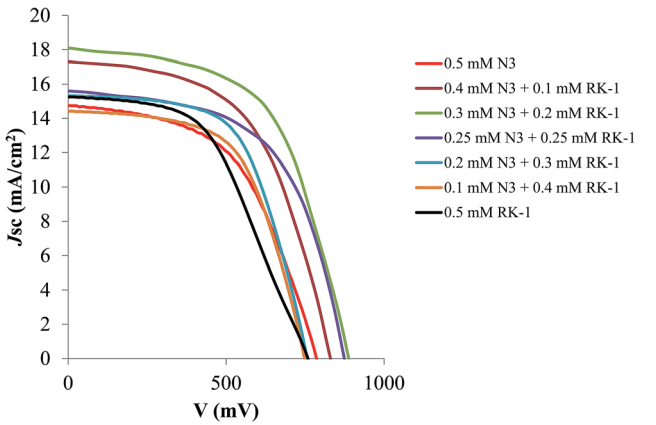

Fig. 3 Current–voltage characteristics of DSSCs studied.

Table 1 Photovoltaic properties of DSSCs

Sample	Composition	J_{sc} (mA cm^{-2})	V_{oc} (V)	FF (%)	η (%)
1	0.5 mM N3	14.747	786	52.65	6.10
2	0.4 mM N3 + 0.1 mM RK-1	17.321	830	55.00	7.91
3	0.3 mM N3 + 0.2 mM RK-1	18.100	888	57.44	9.23
4	0.25 mM N3 + 0.25 mM RK-1	15.602	828	56.32	7.71
5	0.2 mM N3 + 0.3 mM RK-1	15.103	756	60.10	6.98
6	0.1 mM N3 + 0.4 mM RK-1	14.423	748	59.410	6.40
7	0.5 mM RK-1	15.256	758	51.430	5.82

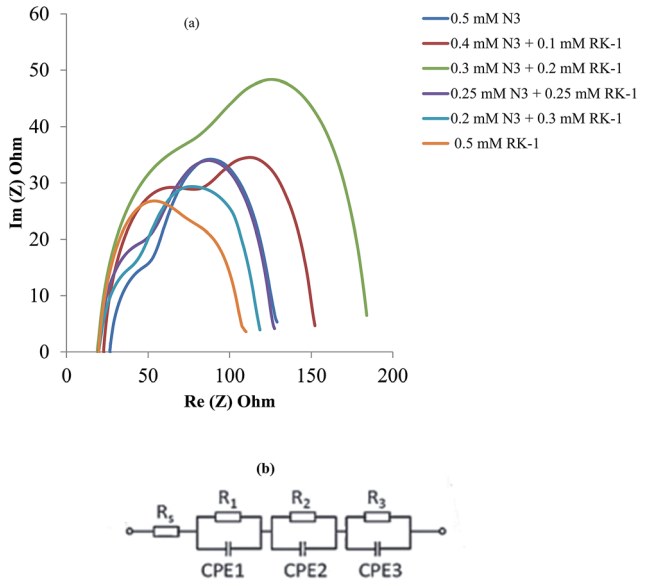

Fig. 4 (a) EIS investigation of DSSCs and (b) equivalent circuit model of the DSSCs in which R_s: serial resistance of FTO glass, $C_1//R_1$: impedance at the CE/electrolyte interface, $C_2//R_2$: impedance at TiO_2/dye/electrolyte interface and $C_3//R_3$: impedance due to the diffusion process of I^-/I_3^- redox couple in the electrolyte (Z_w).

the electrolyte (Z_w).[35,36] The corresponding equivalent circuit is shown in Fig. 4b. Only the first and second arcs appear in the Nyquist plots as shown in Fig. 4a. It is probable that the third arc is overshadowed by second semicircle representing R_2.[37,38] R_2 is related to the charge recombination rate, *e.g.*, a larger R_2 indicates a slower charge recombination and a longer electron lifetime. It can be clearly seen from Fig. 4a that the radii of the semicircles for the co-sensitized DSSCs are much greater than that for the DSSCs based on individual dyes, which indicates a slower charge recombination and a longer electron lifetime. Table 2 shows the R_{ct} values of solar cells. It shows that the R_{ct} value increases upon co-sensitization up to 0.3 mM N3 + 0.2 mM RK-1 and then decreases. Retardation of charge recombination caused by the co-sensitization resulted in an increase in electron lifetime. As a consequence, an improvement of open-circuit photovoltage (V_{oc}) was achieved. The improvement in the photovoltage due to increase charge recombination resistance upon co-sensitization is in the order of sample-3 (R_{ct} = 136 ohm and V_{oc} = 888 mV) > sample-2 (R_{ct} = 96 ohm and V_{oc} = 830 mV) > sample-4 (R_{ct} = 88 ohm and V_{oc} = 828 mV) > sample-5 (R_{ct} = 82.5 ohm and V_{oc} = 756 mV) > sample-6 (R_{ct} = 81.02 ohm and V_{oc} = 748 mV). The longer electron lifetime for the DSSC based on co-sensitization may be either due to a higher surface coverage by the dye on the TiO_2 surface that blocks the approach of I_3^- to the free TiO_2 surface, which decreases the recombination of injected electrons with I_3^- ions, or to a lower aggregation of individual dyes under co-sensitized conditions leading to an improvement of electron injection.

Table 2 Charge combination resistance at TiO_2/dye/electrolyte interface of DSSCs

Sample	Composition	R_{ct} (ohm)
1	0.5 mM N3	83.66
2	0.4 mM N3 + 0.1 mM RK-1	96.00
3	0.3 mM N3 + 0.2 mM RK-1	136.8
4	0.25 mM N3 + 0.25 mM RK-1	88.66
5	0.2 mM N3 + 0.3 mM RK-1	82.85
6	0.1 mM N3 + 0.4 mM RK-1	81.02
7	0.5 mM RK-1	80.12

4. Conclusion

The homogenously mixed solutions of N3 and RK-1 in methanol were used for the co-sensitization of photoanodes of DSSCs. The results indicate that the methanol solutions of N3 + RK-1 show much more intensive and broader bands as compared to N3 dye alone due to the synergistic effect of two dyes. The absorption spectra of co-sensitized TiO_2 films become more intense and broader than the individual dyes. The EIS data indicates a reduced recombination of injected electrons with the tri-iodide ions and a longer electron lifetime. As a consequence, an improvement of open-circuit photovoltage (V_{oc}) is achieved. Under optimal conditions, the power conversion efficiency of 9.23% is reached, which is 34% and 37% higher than those based on individual dyes, N3 (6.10) and RK-1 (5.82), respectively. In conclusion, the improvement in efficiency is mainly due to an increase in J_{sc} (18.1) mA cm^{-2} and V_{oc} (888 mV). The increase in J_{sc} and V_{oc} are strongly correlated to enhance light absorption and reduced charge recombination, respectively.

Acknowledgements

The authors acknowledge the support provided by CoRE-RE, RI of KFUPM.

References

1 K. W. J. Barnham, M. Mazzer and B. Clive, *Nat. Mater.*, 2006, **5**, 161–164.
2 C. J. Brabec, *Sol. Energy Mater. Sol. Cells*, 2004, **83**, 273–292.
3 B. V. S. R. Umer Mehmood, S.-U. Rahman, K. Harrabi and I. A. Hussein, *Adv. Mater. Sci. Eng.*, 2014, **2014**, 12.
4 M.-Q. Yang, N. Zhang, M. Pagliaro and Y.-J. Xu, *Chem. Soc. Rev.*, 2014, **43**, 8240–8254.

5 X. Xie, K. Kretschmer and G. Wang, *Nanoscale*, 2015, **7**, 13278–13292.
6 William A. Vallejo L., Cesar A. Quiñones S. and Johann A. Hernandez S., *Solar Cells - Dye-Sensitized Devices*, InTech, 2011.
7 J. G. Canadell, C. le Quéré, M. R. Raupach, C. B. Field, E. T. Buitenhuis, P. Ciais, T. J. Conway, N. P. Gillett, R. A. Houghton and G. Marland, *Proc. Natl. Acad. Sci. U. S. A.*, 2007, **104**, 18866–18870.
8 M. Hosenuzzaman, N. A. Rahim, J. Selvaraj, M. Hasanuzzaman, A. B. M. A. Malek and A. Nahar, *Renewable Sustainable Energy Rev.*, 2015, **41**, 284–297.
9 U. Mehmood, I. A. Hussein, K. Harrabi, M. B. Mekki, S. Ahmed and N. Tabet, *Sol. Energy Mater. Sol. Cells*, 2015, **140**, 174–179.
10 U. Mehmood, I. A. Hussein, M. Daud, S. Ahmed and K. Harrabi, *Dyes Pigm.*, 2015, **118**, 152–158.
11 U. Mehmood, I. A. Hussein, K. Harrabi and B. V. S. Reddy, *J. Photonics Energy*, 2015, **5**, 053097.
12 A. Hagfeldt, G. Boschloo, L. Sun, L. Kloo and H. Pettersson, *Chem. Rev.*, 2010, **110**, 6595–6663.
13 U. Mehmood, S. Ahmed, I. A. Hussein and K. Harrabi, *Electrochim. Acta*, 2015, **173**, 607–612.
14 S.-Q. Fan, C. Kim, B. Fang, K.-X. Liao, G.-J. Yang, C.-J. Li, J.-J. Kim and J. Ko, *J. Phys. Chem. C*, 2011, **115**, 7747–7754.
15 L. Wei, Y. Yang, R. Fan, Y. Na, P. Wang, Y. Dong, B. Yang and W. Cao, *Dalton Trans.*, 2014, **43**, 11361–11370.
16 Y. Ogomi, S. S. Pandey, S. Kimura and S. Hayase, *Thin Solid Films*, 2010, **519**, 1087–1092.
17 H. Ozawa, R. Shimizu and H. Arakawa, *RSC Adv.*, 2012, **2**, 3198.
18 L. Wei, Y. Yang, R. Fan, P. Wang, L. Li, J. Yu, B. Yang and W. Cao, *RSC Adv.*, 2013, **3**, 25908.
19 S. P. Singh, M. Chandrasekharam, K. S. V. Gupta, A. Islam, L. Han and G. D. Sharma, *Org. Electron.*, 2013, **14**, 1237–1241.
20 A. Yella, H.-W. Lee, H. N. Tsao, C. Yi, A. K. Chandiran, M. K. Nazeeruddin, E. W.-G. Diau, C.-Y. Yeh, S. M. Zakeeruddin and M. Grätzel, *Science*, 2011, **334**, 629–634.
21 C.-M. Lan, H.-P. Wu, T.-Y. Pan, C.-W. Chang, W.-S. Chao, C.-T. Chen, C.-L. Wang, C.-Y. Lin and E. W.-G. Diau, *Energy Environ. Sci.*, 2012, **5**, 6460.
22 H.-P. Wu, Z.-W. Ou, T.-Y. Pan, C.-M. Lan, W.-K. Huang, H.-W. Lee, N. M. Reddy, C.-T. Chen, W.-S. Chao, C.-Y. Yeh and E. W.-G. Diau, *Energy Environ. Sci.*, 2012, **5**, 9843.
23 J. N. Clifford, A. Forneli, H. Chen, T. Torres, S. Tan and E. Palomares, *J. Mater. Chem.*, 2011, **21**, 1693.
24 M. Kimura, H. Nomoto, N. Masaki and S. Mori, *Angew. Chem., Int. Ed. Engl.*, 2012, **51**, 4371–4374.
25 L. Jin, Z. L. Ding and D. J. Chen, *J. Mater. Sci.*, 2013, **48**, 4883–4891.
26 D. Kuang, P. Walter, F. Nüesch, S. Kim, J. Ko, P. Comte, S. M. Zakeeruddin, M. K. Nazeeruddin and M. Grätzel, *Langmuir*, 2007, **23**, 10906–10909.
27 J.-H. Yum, S.-R. Jang, P. Walter, T. Geiger, F. Nüesch, S. Kim, J. Ko, M. Grätzel and M. K. Nazeeruddin, *Chem. Commun.*, 2007, 4680–4682.
28 Z. Wu, J. K. J. van Duren, Z. An, X. Chen and P. Chen, *Bull. Korean Chem. Soc.*, 2014, **35**, 6.
29 J. Chang, C.-P. Lee, D. Kumar, P.-W. Chen, L.-Y. Lin, K. R. J. Thomas and K.-C. Ho, *J. Power Sources*, 2013, **240**, 779–785.
30 G. D. Sharma, G. E. Zervaki, P. A. Angaridis, A. Vatikioti, K. S. V. Gupta, T. Gayathri, P. Nagarjuna, S. P. Singh, M. Chandrasekharam, A. Banthiya, K. Bhanuprakash, A. Petrou and A. G. Coutsolelos, *Org. Electron.*, 2014, **15**, 1324–1337.
31 M. K. Nazeeruddin, S. M. Zakeeruddin, R. Humphry-Baker, M. Jirousek, P. Liska, N. Vlachopoulos, V. Shklover, C.-H. Fischer and M. Grätzel, *Inorg. Chem.*, 1999, **38**, 6298–6305.
32 S. Haid, M. Marszalek, A. Mishra, M. Wielopolski, J. Teuscher, J.-E. Moser, R. Humphry-Baker, S. M. Zakeeruddin, M. Grätzel and P. Bäuerle, *Adv. Funct. Mater.*, 2012, **22**, 1291–1302.
33 A. Eisfeld and J. S. Briggs, *Chem. Phys.*, 2006, **324**, 376–384.
34 K. Sayama, S. Tsukagoshi, T. Mori, K. Hara, Y. Ohga, A. Shinpou, Y. Abe, S. Suga and H. Arakawa, *Sol. Energy Mater. Sol. Cells*, 2003, **80**, 47–71.
35 K. Lee, C. Hu, H. Chen and K. Ho, *Sol. Energy Mater. Sol. Cells*, 2008, **92**, 1628–1633.
36 Y.-L. Xie, Z.-X. Li, Z.-G. Xu and H.-L. Zhang, *Electrochem. Commun.*, 2011, **13**, 788–791.
37 S. Li, Y. Lin, W. Tan, J. Zhang, X. Zhou, J. Chen and Z. Chen, *Int. J. Miner., Metall. Mater.*, 2010, **17**, 92–97.
38 A. S. Nair, R. Jose, Y. Shengyuan and S. Ramakrishna, *J. Colloid Interface Sci.*, 2011, **353**, 39–45.